Published in final edited form as:
Cell Host Microbe. 2009 September 17; 6(3): 253–267. doi:10.1016/j.chom.2009.08.005.

DupA: a key regulator of the amoebal MAP kinase response to *Legionella pneumophila*

Zhiru Li[2,#], **Aisling S. Dugan**[2], **Gareth Bloomfield**[3,4], **Jason Skelton**[4], **Alasdair Ivens**[4], **Vicki Losick**[2,¶], and **Ralph R. Isberg**[1,2,*]

[1]Howard Hughes Medical Institute, Tufts University School of Medicine, 150 Harrison Ave., Boston, MA 02111

[2]Department of Molecular Biology and Microbiology, Tufts University School of Medicine, 150 Harrison Ave., Boston, MA 02111

[3]MRC Laboratory of Molecular Biology, Hills Rd., Cambridge CB2 OQH, UK

[4]Wellcome Trust Sanger Institute, Hinxton CB10 1SA, United Kingdom

SUMMARY

The *dupA* gene, encoding a putative tyrosine kinase/dual specificity phosphatase (Dusp), was identified in a screen for *Dictyostelium discoideum* mutants altered in supporting *Legionella pneumophila* intracellular replication. The absence of *dupA* resulted in hyperphosphorylation of ERK1, consistent with the loss of a phosphatase activity, as well as degradation of ERK2. ERK1 hyperphosphorylation mimicked the response of this protein after bacterial challenge of wild type amoebae. Similar to Dusps in higher eukaryotic cells, the amoebal *dupA* gene was induced after bacterial contact, indicating a response of Dusps that is conserved from amoebae to mammals. A large set of genes was misregulated in the *dupA*$^{-}$ mutant that largely overlaps with genes responding to *L. pneumophila* infection. Some of the amoebal genes appear to be involved in a response similar to innate immunity in higher eukaryotes, indicating there was misregulation of a conserved response to bacteria.

INTRODUCTION

Legionella pneumophila is a facultative intracellular bacterium that causes Legionnaires' disease, initiated after inhalation of aerosols from contaminated water supplies (Marston et al., 1994). The ability of *L. pneumophila* to cause disease is dependent on its ability to modulate the biogenesis of its replication vacuole and grow within host cells. After avoidance of the host cell endocytic pathway, the *Legionella*-containing vacuole (LCV) matures into an endoplasmic reticulum (ER)-like compartment (Swanson and Isberg, 1995). Formation of the LCV requires the function of the *L. pneumophila* Dot/Icm type IV secretion system, a 27 protein complex that translocates a large number of protein substrates into the host cell (Nagai et al., 2002). It is believed that amoebae, such as *Hartmannella vermiformis* and *Acanthamoeba castellanii* (Henke and Seidel, 1986), maintain the reservoir for bacteria that come in contact with the

*Corresponding Author. ralph.isberg@tufts.edu, Phone: 617 636-3993. FAX: 617 636–0337.
[#]Present Address: New England BioLabs, Division of Parasitology, 240 County Road, Ipswich, MA 01938, USA
[¶]Present address: Department of Embryology, Carnegie Institution, Baltimore, MD 21218

human population. Replication of the bacteria within amoebae appears to require a similar, although not identical, set of bacterial proteins as those involved in growth within macrophages (Gao et al., 1997; Segal and Shuman, 1999).

Several host proteins have been identified that contribute to *L. pneumophila* replication. These include factors involved in secretory traffic and ER dynamics, such as vesicle budding factors Sar1 and Arf1 (Kagan et al., 2004) as well as the fusion and tethering factor Rab1 (Kagan et al., 2004). In addition, lowered expression of the amino acid transporter *slc1a5* interferes with *L. pneumophila* growth (Wieland et al., 2005). Most of the studies that have identified these factors have targeted a subset of proteins for analysis. Thus, the total repertoire of host proteins that modulate intracellular growth is unknown.

Dictyostelium discoideum has been used as a model to dissect the amoebal factors that modulate intracellular growth because there are extensive genetic tools available for this organism. *D. discoideum* is a free-living organism that has both a vegetative amoebal stage and a dormant stage. Using the amoebal stage of the organism, it has been shown that *L. pneumophila* trafficking to an ER-bound compartment appears identical to that in macrophages and other amoebal species (Fajardo et al., 2004; Hagele et al., 2000; Lu and Clarke, 2005; Solomon et al., 2000). Furthermore, the global transcriptional response of *D. discoideum* to *L. pneumophila* also bears some similarity to that observed in higher cells (Farbrother et al., 2006). Various classes of stress response genes are induced in response to the *L. pneumophila*, with upregulation of genes encoding proteins associated with ubiquitin-dependent degradation processes. A variety of *D. discoideum* mutants defective in cytoskeletal functions show increased yields of *L. pneumophila* relative to wild type amoebae (Hagele et al., 2000; Solomon et al., 2000; Weber et al., 2006). Similarly, there is enhanced replication in amoeba having disrupted Nramp1 (Peracino et al., 2006), consistent with this channel acting as an active antimicrobial protein. Analysis of *D. discoideum* interactions with another intracellular microorganism, *Mycobacterium marinum*, have uncovered host factors involved replication vacuole maintenance as well as a novel pathway for cell-to-cell spread of the microorganism (Hagedorn et al., 2009; Hagedorn and Soldati, 2007).

In the following study, we performed a non-targeted screen for *D. discoideum* mutants that have altered ability to support *L. pneumophila* growth. Among the mutants identified was an insertion in the gene for a putative tyrosine kinase/dual specificity phosphatase, which we call *dupA*.

RESULTS

Identification of *D. discoideum* mutants with altered susceptibility to *L. pneumophila* infection

The strategy for isolation of *D. discoideum* mutants altered in support of *L. pneumophila* growth is diagramed in Fig. 1. Individual Restriction Enzyme Mediated Insertion (REMI) strains were challenged with *L. pneumophila*-GFP at MOI=0.1 for 72 hours (Experimental Procedures). Wells containing the live cells were then visually screened using fluorescence microscopy and quantitive analysis of captured images (Fig. 1). Out of about 7000 original mutants screened, 10 reproducibly yielded *Legionella*-containing vacuoles (LCVs) that were altered relative to wild type AX4. These alterations were in the size and number of LCVs present as well as the density of bacteria within the LCV, based on quantitation of fluorescent foci of bacterial replication in grabbed images (Figs. 1, 2A). Ten mutants exhibiting a significant change in *L. pneumophila* growth were chosen for further investigation. Additional mutants with subtle enhancement of growth of *L. pneumophila* were observed, but due to their mild phenotype, they were not analyzed further.

Representative fluorescence images of 5 mutants incubated with *L. pneumophila*-GFP for 72 hrs are shown in Fig. 2A. Compared to growth in the wild type AX4 strain, mutant strains RI4 and RI11 contained greater numbers of LCVs (Fig. 2B, quantitative analysis) that were also larger in volume based on increased pixel area (Fig. 2C, quantitative analysis), while mutant strains RI18 and RI10 contained fewer, but larger phagosomes (Fig. 2B,C). In contrast, the F6 mutation in strain RI6 showed fewer and dimmer *L. pneumophila* phagosomes than those in AX4 cells (Fig. 2A–C). Measurement of intracellular growth rates over a 3 day period showed a correspondence to the visual assays, with the yield of bacteria in the RI6 strain at least 10X lower than AX4 (Fig. 2D).

Identification of sites disrupted by REMI

The integration site of the mutations was determined (Experimental Procedures) and the resulting products were searched versus DictyBase.org ((Chisholm et al., 2006; Eichinger et al., 2005)). Southern blotting confirmed that there was only a single insertion of the plasmid into the genome for each of the mutants (data not shown). Of the six mutants mapped, three showed enhanced intracellular growth and will be detailed elsewhere (Fig. 1; strains RI4, RI11, RI18). Of the three that showed depressed growth, one was a predicted transmembrane protein with a haemaglutinnin repeat (strain RI1). The second (strain RI20) had a mutation in gene predicted to encode a regulator of heterotrimeric G protein signaling (RGS18), resulting in a modest reduction *L. pneumophila* intracellular growth (Fig. 1).

The third mutant, F6 (strain RI6), had a plasmid insertion site that was mapped to an Orf that predicted to encode a eukaryotic protein kinase (ePK) domain (E = 6.5e-19) and a downstream dual-specificity protein phosphatase (Dsp) domain (E=1e-27; Finn et al., 2008). As the gene predicts two functional domains, the putative protein will be referred to as DupA (dual role protein A) and the strain RI6 REMI insertion mutant called *dupA(F6).* Interestingly, the mutant also was defective for supporting intracellular growth of *Mycobacterium marinum,* another intravacuolar pathogen (Supplemental Fig. 1).

To confirm the connection between the absence of the *dupA* gene and increased resistance to *L. pneumophila* infection, a complete *dupA*$^{-}$ deletion mutant was constructed (Experimental Procedures). The deletion of the *dupA* gene was examined by genomic DNA PCR, which showed the predicted deletion, and qRT-PCR which showed that there was no detectable expression of *dupA* (data not shown). When the *ΔdupA*$^{-}$ mutant was challenged with *L. pneumophila*, the phenotype of the deletion mutant appeared very similar to the REMI insertion (Fig. 3B). In each case, there were fewer viable, cell-associated bacteria at early timepoints, followed by a period of growth kinetics similar to wild type. Bacterial replication, however, eventually slowed relative to the wild type AX4 strain. We attempted to isolate a full-length *dupA* gene to perform complementation analysis, but we were unable to isolate an intact expressed gene. Instead, fragments containing the Dsp domain, the kinase domain, or both were expressed in *D. discoideum.* None of the partial gene fragments could complement the mutation. Nevertheless, the ability to reconstruct the mutant phenotype using an independent strategy is consistent with depressed intracellular replication of *L. pneumophila* being the result of *dupA* deletion.

DupA is necessary for *D. discoideum* development

The *dupA*$^{-}$ mutants displayed slower growth rates in axenic medium than did wild type and grew as microcolonies, instead of spreading evenly on tissue culture plates as seen with AX4 cells (compare Figs. 3C and 3D). When *D. discoideum* AX4 and *dupA(F6)* cells were plated on the bacterial lawn of *Klebsiella aerogenes* AM2515, both strains could form plaques. However, unlike AX4 cells, the *dupA(F6)* mutant could not form fruiting bodies. To gain insight into the developmental defect of the mutant, a standard development assay was

performed on a solid substrate (Experimental Procedures). AX4 cells formed fruiting bodies typical for a wild type strain after 30 hr incubation (Fig. 3E). In contrast, *dupA(F6)* cells were arrested at the pre- aggregation stage, the initial event in development of fruiting bodies (Fig. 3F).

The absence of DupA leads to increased phosphorylation of *Dictyostelium* ERK1

The Dsp domain of DupA indicates that DupA may function as a dual specificity phosphatase for a MAP kinase. *Dictyostelium* has two MAPKs similar to members of the mammalian ERK family: ERK1 and ERK2. Elimination or overexpression of each of these ERK proteins results in developmental and/or chemotactic defects (Segall et al., 1995; Sobko et al., 2002). The similarity of the developmental defects of the *dupA*$^{-}$ and ERK overexpression prompted us to determine if MAP kinases are possible targets of DupA, by measuring phosphorylation levels of the *D. discoideum* ERKs.

The levels of ERK phosphorylation in *dupA*$^{-}$ mutant cells were examined by anti-phospho-ERK antibody directed against Thr202/Tyr204 of human p44 MAP kinase (Experimental Procedures; (Maeda et al., 2004)). There were small amounts of a species predicted to comigrate with phospho-ERK1 protein in vegetatively growing AX4 cells (Fig. 4A; AX4), consistent with previous reports (Sobko et al., 2002). In contrast, a much higher level (>15 fold) of phospho-ERK1 was detected in *dupA*$^{-}$ cells (Fig. 4A; *dupA*). To confirm that ERK1 was the protein that was highly phosphorylated in *dupA*$^{-}$ cells, we expressed Myc tagged *D. discoideum* ERK1 on a plasmid. The Myc-tagged ERK1 showed a phosphorylated band that migrated slightly slower than ERK1(Fig. 4A; AX4 pErk1-Myc) with significantly more phosphorylation of the mycERK1 band in *dupA*$^{-}$ cells (*dupA*$^{-}$ pErk1-Myc). Similar results were observed with the *ΔdupA* strain. In contrast to ERK1, the anti-phospho-ERK reacting band that comigrated with the predicted molecular weight of ERK2 totally disappeared in the *dupA*$^{-}$ strain (Fig. 4B). The absence of this species apparently resulted from degradation, as stripped blots showed there was a loss of the comigrating band that cross-reacted with anti-human ERK2 (Fig. 4B), in spite of the fact that transcription of *erk2* in the *dupA*$^{-}$ mutant appeared to be normal (P =1; www.ebi.ac.uk/arrayexpress, accession # E-TABM-509).

To investigate whether the hyperactivation of ERK1 observed in the *dupA*$^{-}$ strain mimics the response of wild type amoebae to bacteria, the phospho-ERK1 level was measured in *D. discoideum* cells in response to *L. pneumophila*. ERK1 was phosphorylated rapidly after contact with *L. pneumophila* (Fig. 4C,E). At 60 min post-infection, maximum phosphorylation of ERK1 was observed, with 12 fold higher activation than prior to infection. The activation of ERK1was transient, as ERK1 phosphorylation returned to low levels by 240 min post-infection (Fig. 4C,E). The *dupA*$^{-}$ mutant cells, in contrast, showed high levels of ERK1 phosphorylation throughout infection, with only a 2 fold increase approximately 30 min after challenge with bacteria (Fig. 4C,E). Even so, at all timepoints there was still more phospho-ERK1 in the *dupA*$^{-}$ mutant than observed in the wild type. The elevated level of phospho-ERK1 in the *dupA*$^{-}$ strain was due to increased phosphorylation of the protein and not due to enhanced expression. Similar to what was observed with ERK2, the *dupA*$^{-}$ strain showed reduced amounts of 70 kDal antigen that comigrated with the hyperphosphorylated band and cross-reacted with anti-ERK (Fig. 4D). This indicates that the fraction of ERK1 that was phosphorylated relative to the pool of ERK1 present in the *dupA*$^{-}$ strain was even higher than displayed in Fig. 4E, which was normalized to unrelated protein levels. These results indicate that ERK1 phosphorylation is negatively regulated by DupA and responds to the interaction between *L. pneumophila* and *D. discoideum*.

The fact that the *dupA*$^{-}$ mutant appears hyperactivated in a fashion that seems to mimic the response to *L. pneumophila* raises the possibility that phosphorylation of ERK1 is the result of a general pathway for recognition of bacteria. To test this idea, the AX4 wild type strain

was challenged either with *L. pneumophila dotA*$^{-}$, which is unable to translocate type IV substrates, or with the laboratory strain *E. coli* K12 (Fig. 4F, G). There was a robust response of ERK1 phosphorylation in AX4 to the *dotA*$^{-}$ mutant that appeared similar in intensity and kinetics to that observed with wt *L. pneumophila* (Fig. 4F), a result that mirrors previous observations with mouse bone marrow macrophages (Shin et al., 2008). Challenge with *E. coli* K12 also caused an increase in ERK1 phosphorylation (Fig. 4G), although the intensity of this response was markedly lower than that observed with *L. pneumophila*. Therefore, ERK1 appears to be phosphorylated in response to multiple strains of bacteria, but the intensity of this response is not uniform.

Expression of *dupA* is induced upon *L. pneumophila* challenge

The defect in intracellular growth exhibited by amoebae deranged for MAPK regulation brings up an important link to the mammalian response to *L. pneumophila*. In a human phagocytic cell line, the dual specificity phosphatases *dusp1*, *dusp2* and *dusp6*, which are negative regulators of the MAPK response, are highly induced genes after *L. pneumophila* challenge (Losick and Isberg, 2006). The phenotype of the *dupA*$^{-}$ mutant indicates that downmodulation by Dusps may be an evolutionarily conserved response to bacteria. The expression of the *dupA* gene in response to *L. pneumophila*, therefore, was carefully examined by analyzing the subset of cells harboring bacteria and comparing them with uninfected cells in the same population. *D. discoideum* AX4 was incubated at low MOI with *L. pneumophila* expressing GFP, the infected GFP positive cells were sorted by flow cytometry and subjected to qPCR (Experimental Procedures: Fig. 4H). Consistent with the results from mammalian cells, the *dupA* gene was induced 10 fold in the infected GFP^{+} *D. discoideum* cells compared to cells from uninfected cultured or to the uninfected sorted GFP^{-} population (Fig. 4I). This is consistent with the notion that downmodulation of MAPK activation is a conserved response to *L. pneumophila*.

Amoebal genes misregulated in absence of DupA are regulated in response to *L. pneumophila* challenge

As the absence of DupA caused constitutive activation of a MAP kinase cascade which should control global regulatory circuits, the transcriptional profile of the *dupA*$^{-}$ mutant was compared to the wild type AX4 in the presence or absence of *L. pneumophila* (Experimental Procedures). The wild type and *dupA*$^{-}$ mutant were challenged with *L. pneumophila* expressing GFP at MOI = 1.0, at 6 h. post-infection cells were collected, and RNA was isolated from infected amoeba as well as uninfected cells otherwise treated identically. The RNA from each sample was used to probe an array of 9320 *D. discoideum* orf segments, and the four conditions were compared to each other (Experimental Procedures). There were three readily apparent properties of these bacterial challenges: A) In wild type amoebae, there was a large transcriptional response to the presence of *L. pneumophila* at 6 hrs. post-infection that involved alterations in genes encoding proteins involved in translation and transcriptional regulation (Fig.5; Table 1; Supplemental Tables 1–6); B) a large cadre of genes induced in the wild type amoebae in response to *L. pneumophila* were overexpressed in the *dupA*$^{-}$ mutant prior to bacterial infection, while many of the genes that were reduced in expression in response to *L. pneumophila* were underexpressed in the *dupA* mutant prior to exposure to bacteria (Fig. 5A; Supplemental Tables 1 and 4); and C) several of the genes that were induced in response to *L pneumophila* and overexpressed in the *dupA*$^{-}$ mutant encoded proteins that show similarity to proteins involved in the innate immune response in higher eukaryotes (Table 1; Supplemental Table 8). To confirm the microarray gene expression, qRT-PCR was used to verify that several of the genes upregulated on the arrays including *tirA, gefN, pdiA, discoidin I, and nod3* were also strongly induced as measured by qRT-PCR. The amount of altered expression was consistent with that observed on the array (Fig. 6A and C).

A. The presence of a large transcriptional response to L. pneumophila— Incubation of the wild type AX4 to *L. pneumophila* for 6 hrs resulted in altered expression of a large number of genes, many of which have been described in a previous microarray study (Farbrother et al., 2006; Supplemental Tables 3 and 6; threshold of 2X change relative to uninfected; $P < 0.05$). As observed previously, there was upregulation of tRNA synthetase genes in response to *L. pneumophila* (Supplemental Table 3). In contrast, almost every ribosomal protein gene was downregulated in response to *L. pneumophila* (Fig. 5D; Supplemental Table 7). Although these may appear to be counterproductive responses, this phenomenon has some similarity to the *E. coli* stringent response, in which the charging status of tRNAs modulates the rate of protein synthesis (Goldman and Jakubowski, 1990).

B. Genes misregulated in the dupA⁻ mutant showed altered expression in wild type AX4 after L. pneumophila challenge—In the absence of added bacteria, the *dupA*⁻ mutant showed altered expression of a large number of genes, many of which were found to be differentially expressed in response to bacterial challenge of the wild type AX4 strain (2-fold cutoff for minimal change; $P<0.05$; Supplementary Tables 2 and 5). 64% of the genes overexpressed in the uninfected *dupA*⁻ mutant were upregulated after *L. pneumophila* was incubated with the wild type amoebae, while 48% of the underexpressed genes were downregulated (Supplementary Tables 3 and 6; Fig. 5A–C). 521 genes that were differentially expressed ($p<0.05$) when AX4 was challenged by *L. pneumophila*-challenged AX4 also showed misregulation in the uninfected *dupA*⁻ mutant when compared to AX4. 244 of these genes were upregulated in both comparisons and 261were downregulated in both comparisons; only 16 genes were significantly upregulated in one comparison and downregulated in the other. This association is far greater than one would expect by chance alone ($p <2.2e-16$, odds ratio = 1249.6; one-tailed Fisher's exact test (R-Development-Core-Team, 2008).

Table 1 shows a summary of an annotated set of genes that were altered in expression in uninfected *dupA*⁻ and which were regulated after challenge of the wild type with *L. pneumophila*. When the *dupA*⁻ mutant was challenged with *L. pneumophila* there was very little change in expression of most of the differentially expressed genes (Table 1; Fig. 5A). Key among the misregulated genes in the *dupA* mutant was an apparent switch in the nature of the protein degradation pathways present in the mutant, with several cysteine and serine proteases underexpressed in the mutant, and enhanced expression of the ubiquitin-proteosome machinery (Table 1; Protein Degradation). These changes predicted the response of the wild type amoebae to *L. pneumophila*, as the proteasome-ubiquitin pathway genes were induced after bacterial challenge.

C. Hyperexpression of genes similar to immune response genes—Several genes that encode proteins with sequence similarities to host innate immune response proteins found in higher eukaryotes were overexpressed in the *dupA* mutant and were upregulated in response to *L. pneumophila* (Table 1). Cosson and Soldati had hypothesized that many of these genes may be involved in the amoebal response to bacteria (Cosson and Soldati, 2008). Most notable, the TIR domain containing protein *tirA* carries out sensor or adaptor functions in the detection of pathogens, and mutations in this gene were previously shown to confer hypersensitivity of *D. discoideum* to high multiplicity infection by *L. pneumophila* (Chen et al., 2007). Another gene associated with this response is *slrA*, encoding a leucine rich repeat (LRR) protein, but it was not differentially expressed by microarray analysis, perhaps due to weak spotting of this gene on the array. As both these proteins appear to be involved in a hypothesized amoebal innate immune response to pathogens (Chen et al., 2007), *tirA* and *slrA* gene expression was carefully monitored in infected wild type *D. discoideum* using qPCR. AX4 cells were incubated with *L. pneumophila*-GFP at MOI= 1.0, and 1h, 4h, 6h or 18h after infection, RNA was isolated from sorted cells harboring fluorescent bacteria. Both the *tirA* and *slrA* genes were induced shortly after *L. pneumophila* infection (Fig. 6A and B). In the case of *tirA*, expression increased

to more than 130 fold compared to the uninfected control at 6h post infection. In the uninfected *dupA*$^{-}$ mutant, there was also overexpression of *tirA* in the absence of bacteria. A similar pattern of induction was also observed for *slrA* gene (Fig. 6B). The induction of *tirA*, *slrA*, as well as other potential immune response genes (Table 1), and their overexpression in the *dupA*$^{-}$ mutant suggest that DupA plays an important role in a putative *D. discoideum* innate immune response by negatively regulating a subset of these genes.

DISCUSSION

We have identified a mutant disrupted in the regulation of a large number of amoebal genes that respond to *Legionella pneumophila* infection. As bacterial replication was reduced in this mutant, the regulatory circuit partially controlled by DupA appears to be an important determinant of the fate of *L. pneumophila* after it encounters amoebae. Furthermore, some common elements of this amoebal response to pathogens may control the intracellular replication of a broad swath of microorganisms, given that the unrelated *Mycobacterium marinum* was defective for either uptake or initiation of replication in *dupA* mutants (Supplementary Fig. 1).

The regulatory circuit controlled by DupA is also evolutionarily conserved. Mutations in *dupA* resulted in hyper-phosphorylation of the *D. discoideum* ERK1 protein as well as apparent degradation of ERK2 (Fig.4A and B). The predicted gene product of *dupA* encodes both a kinase and a dual specificity phosphatase domain (Dsp), making it the most likely candidate to be the direct negative regulator of ERK1 that is missing in the mutant. Although we do not know that the DupA phosphatase domain acts directly on ERK1, there is likely to be at least one important phosphatase activity that is misregulated in the mutant, as a large number of organisms use Dusps as the primary negative regulators of MAP kinases (Camps et al., 2000). Consistent with a function that is similar to Dusps in higher eukaryotes, the DupA gene was shown to be upregulated in the wild type *D. discoideum* AX4 in response to *L. pneumophila* infection (Fig. 4I). This is identical to observations in mammalian cells, in which three of the most highly upregulated genes in response to *L. pneumophila* are MAP kinase phosphatases (Losick and Isberg, 2006).

At least some of the phenotypic changes associated with the *dupA*$^{-}$ mutant can be attributed to hyperphosphorylation of ERK1. We have analyzed a *D. discoideum* strain that overproduces a constitutively active MEK1 protein, which causes hyperphosphorylation of ERK1 (Sobko et al., 2002) and has no effect on ERK2 phosphorylation or stability (Supplemental Fig. 2). Intracellular growth of *L. pneumophila* was mildly reduced in such a strain, but this result is tempered by the fact that ERK1 phosphorylation levels were significantly lower in the constitutively active strain than in the *dupA*$^{-}$ mutant (Supplemental Fig. 2). Furthermore, we were unable to demonstrate that the phosphorylation phenotype was due to overproduction of MEK1 rather than due to constitutive activity (Supplemental Fig. 2). At any rate, this result is consistent with ERK1 hyperactivation interfering with intracellular growth, but does not eliminate the possibility that loss of ERK2 or an uncharacterized property of the *dupA*$^{-}$ mutant make additional contributions to this phenotype.

Although in the *dupA*$^{-}$ mutant there was altered regulation of a large group of proteins that respond to *L pneumophila* infection, this did not result in an absolute block on intracellular growth. It is not clear that in every instance, the consequence of the altered gene expression is intended to restrict the pathogen. For instance, there appears to be global reduction of ribosomal protein gene expression after *L. pneumophila* challenge of wild type (Fig. 5C; Supplemental Table 7). This is similar to what was observed in a previous array analysis of *D. discoideum* challenged with *L. pneumophila* (Farbrother et al., 2006), but very different from the response of *D. discoideum* to *E. coli* (Sillo et al., 2008). Slowing ribosomal protein synthesis in host

cells, which probably leads to slowed growth of the amoebae, may be a response to intracellular pathogens that is counterproductive for the amoebae. In support of this point, *L. pneumophila* growth within *D. discoideum* is enhanced in suboptimal growth medium or by plating amoebae at high culture densities (Solomon et al., 2000; E. Chen and R. Isberg, unpublished). Furthermore, *L. pneumophila* encodes several Dot/Icm translocated substrates that interfere with host protein synthesis, possibly blocking the host cell cycle (Belyi et al., 2008;Kubori et al., 2008). Therefore, the *dupA*$^{-}$ mutation causes a deranged amoebal response to pathogens, with the consequence that the sum of transcriptional activity of the host cell does not efficiently support intracellular growth under the conditions tested.

The MAP kinase signaling pathways in *D. discoideum* are simplified versions of what is found in mammals, with ERK1 and ERK2 being the only terminal kinases. ERK2 is involved in oscillatory cAMP signaling during development (Segall et al., 1995), while ERK1 controls events associated with chemotaxis and aggregation (Goldberg et al., 2006; Mendoza et al., 2007). In parallel to the work described here, it has been demonstrated that mouse macrophages challenged with *L. pneumophila* undergo phosphorylation of multiple MAPKs (Shin et al., 2008). Interestingly, the pattern of ERK phosphorylation in macrophages is reminiscent of our observations, as activation of ERK is independent of the *dot*/*icm* system. Surprisingly, the response in macrophages also did not require known pattern recognition receptors. Perhaps there is an evolutionarily conserved response to bacterial adhesion that is shared in both amoebae and mammalian cells that modulates microbial interaction. The ability of the pathogen either to manipulate or defend against such host responses in amoebae could be one of the critical selective pressures that also allow bacterial survival and growth in mammalian phagocytic cells.

A number of genes that may encode a primitive amoebal innate immune response showed altered expression in response to *L. pneumophila*, and many of these are misregulated in the *dupA*$^{-}$ mutant. Most striking is the altered regulation of the *slrA*, *tirA* and *tirC* genes (Chen et al., 2007; Sillo et al., 2008; O'Neill and Bowie, 2007). It has been previously reported that *tirA* expression was increased 16 fold in newly identified Sentinel Cells, which are hypothesized to be immune-like cells generated by the slug form of amoebae (Chen et al., 2007). Furthermore, *D. discoideum tirA*$^{-}$ is more sensitive than wild type to killing after high multiplicity challenge with *L. pneumophila*, indicating that the protein may promote enhanced cell survival in the presence of bacteria (Chen et al., 2007). Consistent with this hypothesized role, we observed a large increase in expression of both *slrA* and *tirA* in amoebae harboring *L. pneumophila*, and *slrA* is severely overexpressed in the *dupA* mutant (Fig. 6). We have found that a *tirA*$^{-}$ mutant still is able to support *L. pneumophila* replication with similar efficiency to wild type strains using low MOI challenge with the bacterium (data not shown). However, the requirement of the *tirA* product for supporting host cell viability in the presence of high doses of pathogen, as well as the regulatory profile of this gene, are properties that are consistent with the protein playing a role in a global response that modulates *D. discoideum* protection from pathogens.

In conclusion, disrupted DupA function is associated with profound misregulation of a group of genes that respond to association of *L. pneumophila* with amoebae. That several of the genes upregulated in response to the bacterium had been suggested previously to encode proteins involved in a form of amoebal innate immunity is consistent with their proposed role in the biology of *D. discoideum*. In fact, this primitive form of immune surveillance may be part of a larger regulatory circuit controlled by ERK1 and DupA. Most intriguing is the possibility that there are important parallels between macrophages and amoebae, the natural host for *L. pneumophila*, as negative control of host cell MAPKs appears to be a conserved response in these disparate cell types worthy of further investigation.

EXPERIMENTAL PROCEDURES

Bacteria strains, plasmids and media

L. pneumophila Lp01 is proficient for intracellular growth and was grown on AYE liquid medium or CYE agar plate (Berger and Isberg, 1993) (Feeley et al., 1979). The GFP-encoding plasmid pAM239 was described previously (Losick and Isberg, 2006). The *L. pneumophila* strains were grown to post-exponential phase (A_{600} = 3.5–4.0), at which time motile bacteria were added to amoebae at the noted multiplicities of infection (MOI). The approximate concentration of bacteria was determined by assuming that A_{600} = 1.0 is equivalent to 10^9 bacteria/ml.

Growth assay of *L. pneumophila* in *D. discoideum*

D. discoideum strains were routinely grown axenically in HL-5 liquid medium (Sussman, 1987) supplemented with penicillin and streptomycin (100 U/ml; GibcoBRL) at 21.5°C. Amoebae in logarithmic stage were prepared by plating 1 to 1.25 × 10^5 cells 2 days prior to use in fresh HL-5 medium. Cells were harvested and washed once with phosphate-buffered saline (PBS) and pelleted for 5 min at 200×*g*, resuspended at 10^6 cells/ml in MB medium (20 mM MES (2 (*N*-morpholino) ethanesulfonic acid) (pH=6.9), 0.7% yeast extract, 1.4% BBL thiotone E peptone). 0.5 ml or 0.1 ml were added to each well in 24-well or 96-well plates prior to incubation at 25.5°C for 2 h. to allow adherence (Solomon et al., 2000) before the bacterial infection. Infections with *L. pneumophila* were performed as described (Solomon et al., 2000).

REMI mutagenesis, mutant mapping and construction of mutants

REMI mutagenesis was performed as described (Kuspa and Loomis, 1992). 1μg of *Bam*HI linearized plasmid pBsrΔBglII (kind gift of Dr. David Knecht, U. Connecticutt, Storrs) and 5units of *Dpn*II were transformed into AX4 cells by two consecutive electroporation pulses (Bio-RAD, USA) at 0.85kv, 25μF, applied 5 seconds apart. Cells were then serially diluted in HL-5 medium to 10 cells per ml and 100μL of cell were plated in tissue culture treated 96-well plate immediately following electroporation. Transformed cells were allowed to recovery for 24 h before selection in HL-5 media containing 5 μg/ml blasticidin S. Drug-resistant cells were collected, counted and plated.

To map the insertion site of plasmid,s we used plasmid rescue or reverse PCR. Plasmid rescue was performed as described (Kuspa and Loomis, 1992). Briefly, DNA from the mutant was digested with *ClaI*, which does not cut the integrated vector, or with another enzyme determined by Southern blot to generate a fragment of <15kB, circularized by ligation, and transformed into *Escherichia coli*. Plasmid DNA isolated from *E. coli* was sequenced commercially with primers: TGAGCGCAACGCAATTAA and CCATTTTTTTTTTTAAAGATTTGATGG that correspond to plasmid sequences. For inverse PCR isolation, 10 μg of genomic DNA from AX4 was treated with restriction enzymes that digest the plasmid close to the end of the insertion position, such as *Afl*III or *Nla*III. The DNA was set up for self-ligation in a volume of 100 μl. One μl of the ligation mix was used for inverse PCR using the 5′ primer CCAATCAATGATAATGATCCTCCC and the 3′primer AAAGTGAATCCTCGACAAG. The resulting sequences were used to BLAST search DictyBase.org (Chisholm et al., 2006; Eichinger et al., 2005).

To knock out the *dupA* gene, 1kb genomic DNA fragments located upstream, Blasticidin S resistance (BSR) cassette and 1kb downstream of the targeted gene were generated by PCR to transform *D. discoideum* AX4 cells as described above. The transformants were selected on blasticidin S for 7 days, single cell cloned, and screened for their phenotypes. The correct insertion of the genomic fragment was determined by DNA sequencing.

D. discoideum screen

Single *D. discoideum* REMI clones in a 96 well microtiter dish were harvested and replated into two 96 well plates having optically clear bottoms (Corning Cat# 3614). *D. discoideum* mutants were incubated with *L. pneumophila* - GFP for 72 h. at MOI=0.1 and individual wells containing infected *D. discoideum* were visually screened using fluorescence microscopy. 3 images were grabbed from each well and inspected later (Fig. 1). Images were analyzed using IP lab software. Segmentation was first applied for each image to separate the target pixels from background pixels. Thresholds for size and brightness of the fluorescence for each LCV were established for AX4 cells and used as a comparison for REMI mutants. Clones that deviated from wild type were retested in triplicate, and were retained for further analysis, as displayed in Fig. 2.

Quantitative PCR

Total RNA was isolated from 10^7 *Dictyostelium* cells using the Qiagen RNeasy mini kit (Qiagen Cat.No. 74104) or Trizol (Invitrogen, Carlsbad, California, United States). The first strand of cDNA were reverse transcribed from 2 μg of DNA-free RNA using the Superscript^{TM} First-strand Synthesis System (Invitrogen) containing DNase/Rnase-free water and buffer suggested by the manufacturer in a total reaction volume of 30 μl. 2 μl of the resulting cDNA reaction mix was then used for real-time quantitative PCR (qPCR) analysis. Quantitative PCR was performed using the GenAmp5700 system with the SYBR Green PCR reagent (Applied Biosystems). For each quantification, triplicate samples were performed in parallel, quantification results were normalized based on the β-actin control and average values were calculated.

D. discoideum development assay

Briefly, 5×10^7 of vegetative cells were harvested by centrifugation at 1000 rpm for 5 min at a density = 1–2 × 10^6 cells/ml and washed twice with PDF buffer (20 mM KCl, 5 mM $MgCl_2$, 20 mM KPO_4, pH=6.2). Cells were resuspended in 500μl of PDF buffer and dispersed on nitrocellulose membrane (Osmonics Inc. E04BG04700) on top of a PDF-soaked pad (Life Sciences, P/N66025). Extra PDF buffer (~500 μl) was added to the side of the Petri dish and left on the bench for 5 min. Cells were then developed at 21.5°C in humid container and observed microscopically.

Western blot analysis and antibodies

To avoid potential post-lysis modification or degradation of proteins of interest, 1×10^6 of *D. discoideum* cells were harvested and pelleted by centrifugation at 1000rpm at 4°C for 5 min and directly lysed in 100 μl of 1×SDS sample buffer followed by heat denaturation at 95°C for 5 min. Total protein extracts were separated by SDS–PAGE electrophoresis. Proteins were then transferred onto a nitrocellulose membrane followed by blotting and probing. For immunoblot quantification, appropriately nonsaturated film exposures were selected and scanned, and the images were quantified by densitometry using a Kodak ImageStation. Anti-ERK (sc-153) was from Santa Cruz Biotechnology. Anti-phospho-p44/42 MAPK (#9101S) was from Cell Signaling Technology. Anti-tubulin was from Serotech (MCA785). All antibodies were used following manufacture's instructions for Western blot.

Micoarray analysis

D. discoideum cells were infected with Lp01 at an MOI=1 for 6 h. and compared to *D. discoideum* in the absence of infection. RNA was then isolated from the cells and prepared for microarray analysis. The RNA samples were prepared by Trizol extraction.

For array analysis, three independent biological experiments were performed infecting wild-type and mutant RI6 (*dupA*(*F6*)) with *L. pneumophila*. 25 μg RNA was extracted and labeled by incorporation of Cy3-or Cy5-conjugated dCTP (GE Healthcare) in a reverse transcription reaction catalyzed by Superscript III (Invitrogen). For each biological replicate, labeled cDNA samples with complementary dyes incorporated were paired so that the comparisons of direct interest were made: WT 0h was paired with WT 6h, WT 0h with mutant 6h, mutant 0h with mutant 6h, and WT 6h with mutant 6h. In this loop design, each sample was labelled twice, once with each dye. In total twelve microarrays were used; four for each biological replicate. The samples thus paired were hybridized to custom DNA microarrays (Bloomfield et al., 2008). Background fluorescence was subtracted from the scanned images (Kooperberg et al., 2002), the data then normalized using the print-tip Loess algorithm, linear models were fitted and the significance of apparent changes in expression was assessed using limma (Smyth, 2004; Smyth et al., 2005). P-values obtained from limma's moderated t statistics were adjusted to control the false discovery rate and genes with adjusted values < 0.05 taken to show significant evidence of differential expression. We filtered the data further to exclude genes with low-magnitude changes using a fold-change cutoff of 2. The array design is available from ArrayExpress (www.ebi.ac.uk/arrayexpress) under the accession A-SGRP-3. The full data for this experiment has been submitted to the same database under the accession E-TABM-509.

Supplementary Material

Refer to Web version on PubMed Central for supplementary material.

Acknowledgments

RI is an Investigator of Howard Hughes Medical Institute. GB, JS and AI were supported by the WellcomeTrust (Grant 06724). We thank Kay Jagels and Theresa Feltwell for microarray support, Fredrik Söderbom for help with *D. discoideum* methods and instructions on performing the aggregation assay and Max Isberg for help with composition of figures. We thank Drs. Vicki Auerbuch Stone, Elizabeth Creasey, Matt Heidtman, Tamara O'Conner, Alex Ensminger and Molly Bergman for review of the text, Dr. Janet Smith for help with anti-P-ERK detection and discussions, Dr. Adam Kuspa for the *tirA* mutant, and Dr. Richard A. Firtel for the ERK1-Myc and MEK plasmids.

References

Belyi Y, Tabakova I, Stahl M, Aktories K. Lgt: a family of cytotoxic glucosyltransferases produced by *Legionella pneumophila*. J Bacteriol 2008;190:3026–3035. [PubMed: 18281405]

Berger KH, Isberg RR. Two distinct defects in intracellular growth complemented by a single genetic locus in *Legionella pneumophila*. Mol Microbiol 1993;7:7–19. [PubMed: 8382332]

Bloomfield G, Tanaka Y, Skelton J, Ivens A, Kay RR. Widespread duplications in the genomes of laboratory stocks of *Dictyostelium discoideum*. Genome Biol 2008;9:R75. [PubMed: 18430225]

Camps M, Nichols A, Arkinstall S. Dual specificity phosphatases: a gene family for control of MAP kinase function. FASEB J 2000;14:6–16. [PubMed: 10627275]

Chisholm RL, Gaudet P, Just EM, Pilcher KE, Fey P, Merchant SN, Kibbe WA. dictyBase, the model organism database for Dictyostelium discoideum. Nucleic Acids Res 2006;34:D423–427. [PubMed: 16381903]

Chen G, Zhuchenko O, Kuspa A. Immune-like phagocyte activity in the social amoeba. Science 2007;317:678–681. [PubMed: 17673666]

Cosson P, Soldati T. Eat, kill or die: when amoeba meets bacteria. Curr Opin Microbiol 2008;11:271–276. [PubMed: 18550419]

Eichinger L, Pachebat JA, Glockner G, Rajandream MA, Sucgang R, Berriman M, Song J, Olsen R, Szafranski K, Xu Q, et al. The genome of the social amoeba Dictyostelium discoideum. Nature 2005;435:43–57. [PubMed: 15875012]

Fajardo M, Schleicher M, Noegel A, Bozzaro S, Killinger S, Heuner K, Hacker J, Steinert M. Calnexin, calreticulin and cytoskeleton-associated proteins modulate uptake and growth of *Legionella pneumophila* in *Dictyostelium discoideum*. Microbiology 2004;150:2825–2835. [PubMed: 15347742]

Farbrother P, Wagner C, Na J, Tunggal B, Morio T, Urushihara H, Tanaka Y, Schleicher M, Steinert M, Eichinger L. *Dictyostelium* transcriptional host cell response upon infection with *Legionella*. Cell Microbiol 2006;8:438–456. [PubMed: 16469056]

Feeley JC, Gibson RJ, Gorman GW, Langford NC, Rasheed JK, Mackel DC, Baine WB. Charcoal-yeast extract agar: primary isolation medium for *Legionella pneumophila*. J Clin Microbiol 1979;10:437–441. [PubMed: 393713]

Finn RD, Tate J, Mistry J, Coggill PC, Sammut SJ, Hotz HR, Ceric G, Forslund K, Eddy SR, Sonnhammer EL, Bateman A. The Pfam protein families database. Nucleic Acids Res 2008;36:D281–288. [PubMed: 18039703]

Gao LY, Harb OS, Abu Kwaik Y. Utilization of similar mechanisms by *Legionella pneumophila* to parasitize two evolutionarily distant host cells, mammalian macrophages and protozoa. Infect Immun 1997;65:4738–4746. [PubMed: 9353059]

Goldberg JM, Manning G, Liu A, Fey P, Pilcher KE, Xu Y, Smith JL. The *Dictyostelium* kinome--analysis of the protein kinases from a simple model organism. PLoS Genet 2006;2:e38. [PubMed: 16596165]

Goldman E, Jakubowski H. Uncharged tRNA, protein synthesis, and the bacterial stringent response. Mol Microbiol 1990;4:2035–2040. [PubMed: 1708437]

Hagele S, Kohler R, Merkert H, Schleicher M, Hacker J, Steinert M. *Dictyostelium discoideum*: a new host model system for intracellular pathogens of the genus *Legionella*. Cell Microbiol 2000;2:165–171. [PubMed: 11207573]

Hagedorn M, Rohde KH, Russell DG, Soldati T. Infection by tubercular mycobacteria is spread by nonlytic ejection from their amoeba hosts. Science 2009;323:1729–1733. [PubMed: 19325115]

Hagedorn M, Soldati T. Flotillin and RacH modulate the intracellular immunity of Dictyostelium to Mycobacterium marinum infection. Cell Microbiol 2007;9:2716–2733. [PubMed: 17587329]

Henke M, Seidel KM. Association between *Legionella pneumophila* and amoebae in water. Isr J Med Sci 1986;22:690–695. [PubMed: 3793452]

Kagan JC, Stein MP, Pypaert M, Roy CR. *Legionella* subvert the functions of rab1 and sec22b to create a replicative organelle. J Exp Med 2004;199:1201–1211. [PubMed: 15117975]

Kooperberg C, Sipione S, LeBlanc M, Strand AD, Cattaneo E, Olson JM. Evaluating test statistics to select interesting genes in microarray experiments. Hum Mol Genet 2002;11:2223–2232. [PubMed: 12217950]

Kubori T, Hyakutake A, Nagai H. *Legionella* translocates an E3 ubiquitin ligase that has multiple U-boxes with distinct functions. Mol Microbiol 2008;67:1307–1319. [PubMed: 18284575]

Kuspa A, Loomis WF. Tagging developmental genes in *Dictyostelium* by restriction enzyme-mediated integration of plasmid DNA. Proc Natl Acad Sci USA 1992;89:8803–8807. [PubMed: 1326764]

Losick VP, Isberg RR. NF-{kappa}B translocation prevents host cell death after low-dose challenge by *Legionella pneumophila*. J Exp Med 2006;203:2177–2189. [PubMed: 16940169]

Lu H, Clarke M. Dynamic properties of *Legionella*-containing phagosomes in *Dictyostelium* amoebae. Cell Microbiol 2005;7:995–1007. [PubMed: 15953031]

Maeda M, Lu S, Shaulsky G, Miyazaki Y, Kuwayama H, Tanaka Y, Kuspa A, Loomis WF. Periodic signaling controlled by an oscillatory circuit that includes protein kinases ERK2 and PKA. Science 2004;304:875–878. [PubMed: 15131307]

Marston BJ, Lipman HB, Breiman RF. Surveillance for Legionnaires' disease. Risk factors for morbidity and mortality. Arch Intern Med 1994;154:2417–2422. [PubMed: 7979837]

Mendoza MC, Booth EO, Shaulsky G, Firtel RA. MEK1 and protein phosphatase 4 coordinate *Dictyostelium* development and chemotaxis. Mol Cell Biol 2007;27:3817–3827. [PubMed: 17353263]

Nagai H, Kagan JC, Zhu X, Kahn RA, Roy CR. A bacterial guanine nucleotide exchange factor activates ARF on *Legionella* phagosomes. Science 2002;295:679–682. [PubMed: 11809974]

O'Neill LA, Bowie AG. The family of five: TIR-domain-containing adaptors in Toll-like receptor signaling. Nat Rev Immunol 2007;7:353–364. [PubMed: 17457343]

Peracino B, Wagner C, Balest A, Balbo A, Pergolizzi B, Noegel AA, Steinert M, Bozzaro S. Function and mechanism of action of *Dictyostelium* Nramp1 (Slc11a1) in bacterial infection. Traffic 2006;7:22–38. [PubMed: 16445684]

Segal G, Shuman HA. *Legionella pneumophila* utilizes the same genes to multiply within *Acanthamoeba castellanii* and human macrophages. Infect Immun 1999;67:2117–2124. [PubMed: 10225863]

Segall JE, Kuspa A, Shaulsky G, Ecke M, Maeda M, Gaskins C, Firtel RA, Loomis WF. A MAP kinase necessary for receptor-mediated activation of adenylyl cyclase in *Dictyostelium*. J Cell Biol 1995;128:405–413. [PubMed: 7844154]

Shin S, Case CL, Archer KA, Nogueira CV, Kobayashi KS, Flavell RA, Roy CR, Zamboni DS. Type IV secretion-dependent activation of host MAP kinases induces an increased proinflammatory cytokine response to Legionella pneumophila. PLoS Pathog 2008;4:e1000220. [PubMed: 19043549]

Sillo A, Bloomfield G, Balest A, Balbo A, Pergolizzi B, Peracino B, Skelton J, Ivens A, Bozzaro S. Genome-wide transcriptional changes induced by phagocytosis or growth on bacteria in *Dictyostelium*. BMC Genomics 2008;9:291. [PubMed: 18559084]

Smyth GK. Linear models and empirical bayes methods for assessing differential expression in microarray experiments. Stat Appl Genet Mol Biol 2004;3 Article3.

Smyth GK, Michaud J, Scott HS. Use of within-array replicate spots for assessing differential expression in microarray experiments. Bioinformatics 2005;21:2067–2075. [PubMed: 15657102]

Sobko A, Ma H, Firtel RA. Regulated SUMOylation and ubiquitination of DdMEK1 is required for proper chemotaxis. Dev Cell 2002;2:745–756. [PubMed: 12062087]

Solomon JM, Rupper A, Cardelli JA, Isberg RR. Intracellular growth of *Legionella pneumophila* in *Dictyostelium discoideum*, a system for genetic analysis of host-pathogen interactions. Infect Immun 2000;68:2939–2947. [PubMed: 10768992]

Sussman, M. Cultivation and synchronous morphogenesis of *Dictyostelium* under controlled experimental conditions. In: Spudich, JA., editor. Methods in Cell Biology. Orlando, FL: Ac. Press; 1987. p. 9-29.

Swanson MS, Isberg RR. Association of *Legionella pneumophila* with the macrophage endoplasmic reticulum. Infect Immun 1995;63:3609–3620. [PubMed: 7642298]

Weber SS, Ragaz C, Reus K, Nyfeler Y, Hilbi H. *Legionella pneumophila* exploits PI(4)P to anchor secreted effector proteins to the replicative vacuole. PLoS Pathog 2006;2:e46. [PubMed: 16710455]

Wieland H, Ullrich S, Lang F, Neumeister B. Intracellular multiplication of *Legionella pneumophila* depends on host cell amino acid transporter SLC1A5. Mol Microbiol 2005;55:1528–1537. [PubMed: 15720558]

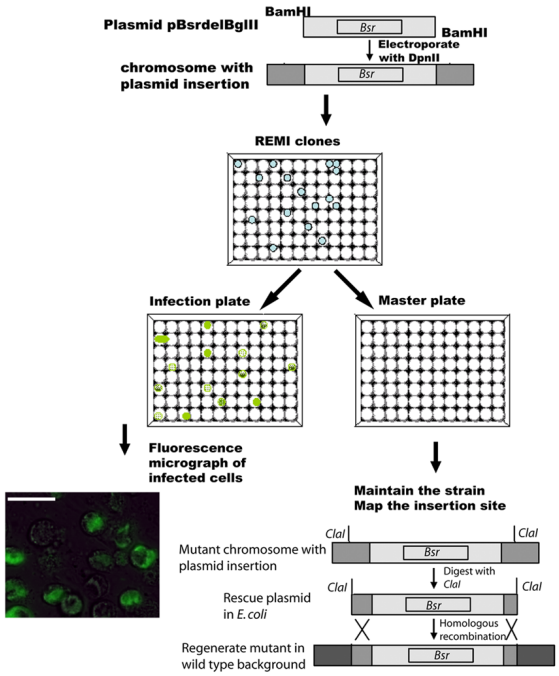

Insertion sites of mutants analyzed in this study

Clone number	Gene disrupted[1]	LCV phenotype[2]	Intracellular Growth[3]	Insertion Site[1]	Protein or ortholog
RI1	*DDB0188806*	Decreased LCVs	Mild growth defect	Chr5: deletion of 3860915- 386279	Haemmaglutinin repeat
RI4	*redA*	Increased number of LCVs	Increased growth	Chr6 : 3581164	*redA* gene; NADPH-cytochrome P450 reductase
RI18	*glk*	Larger individual LCVs	Increased growth	Chr5 : 532508 (upstream of *glk*)	ADP-dependent glucokinase family
RI20	*DDB0218860*	Fewer LCVs	Little change in growth	Chr4 : 4863892	Regulator of G-protein signaling RGS18
RI11	*DDB0231105*	More densely packed LCVs	Increased growth	Chr6: 2786470	HssA/2C/7E family protein
RI6	*DDB0231326*	Fewer LCVs; Less densely packed	Decreased growth	Chr2:7428116	Protein kinase and dual-specificity domains

Figure 1. *D. discoideum* mutants altered in supporting *L. pneumophila* intracellular replication

REMI mutants were plated on optically clear 96 well plates and challenged with *L. pneumophila*-GFP at MOI = 0.1 (green; Scale Bar: 10μ). Image capture was performed after 72 hrs incubation. The mutations were then rescued, transformed into *E. coli*, and regenerated by retransforming into AX4 (Experimental Procedures). [1]Site of insertion was determined by sequencing the joint between the REMI insertion and the chromosome. [2] Growth alteration was determined by performing 96 hour growth curves, plating for viable colonies.

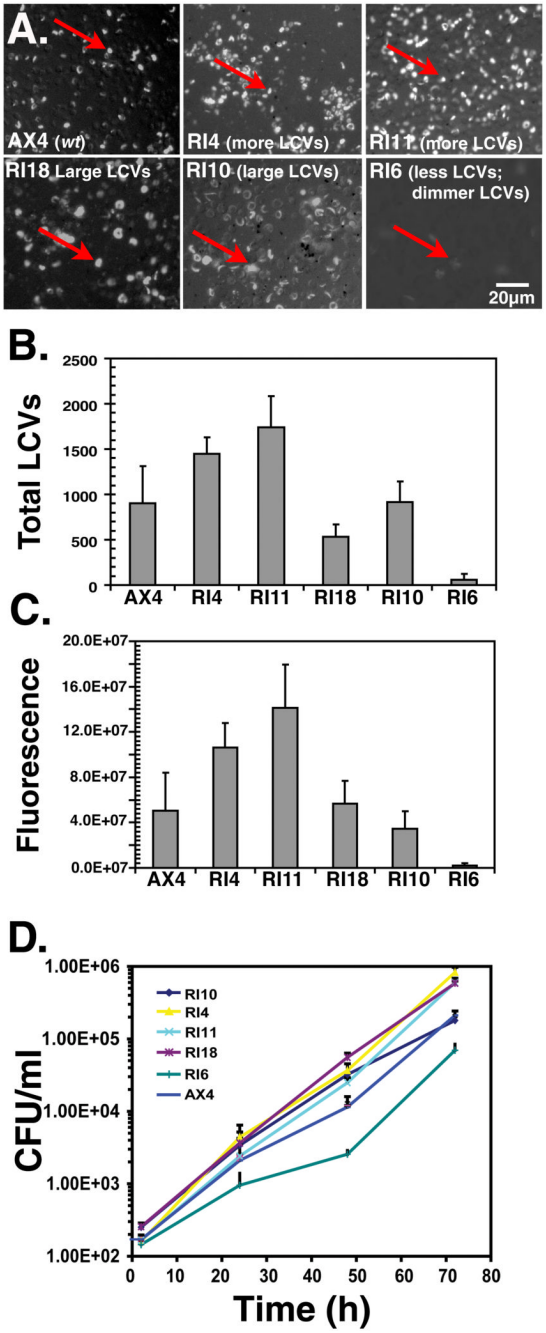

Figure 2. *D. discoideum* REMI mutants altered in bacterial growth show a spectrum of phenotypes

(A) Representative fluorescence micrographs (20X) of REMI mutants after 72 hr. incubation with *L. pneumophila*. AX4 is the parental wild type strain and RI4, RI11, RI18, RI10, RI6 are REMI mutants. Arrows show representative *L. pneumophila* phagosomes. **(B)** REMI mutants alter the number of *Legionella*-containing vacuoles (LCVs) compared to wild type amoebae. Images (20X) of noted REMI mutants challenged with *L. pneumophila*-GFP for 72 hrs. were captured as in (A), and fluorescent foci were quantitated (Experimental Procedures). Each fluorescent focus was defined as a single LCV. Shown are the mean ± SD for triplicate infections. (C). REMI mutants show alterations in yield of intracellular *L. pneumophila*. Images grabbed in panel (B) were used to determine the yield of bacteria. (D). Intracellular growth of

wild-type *L. pneumophila* in REMI mutants. The number of viable bacteria was determined by plating supernatants of lysed *D. discoideum* onto CYE plates at the denoted times and counting CFU (Experimental Procedures). Plotted is the mean CFU from triplicate samples ± SD.

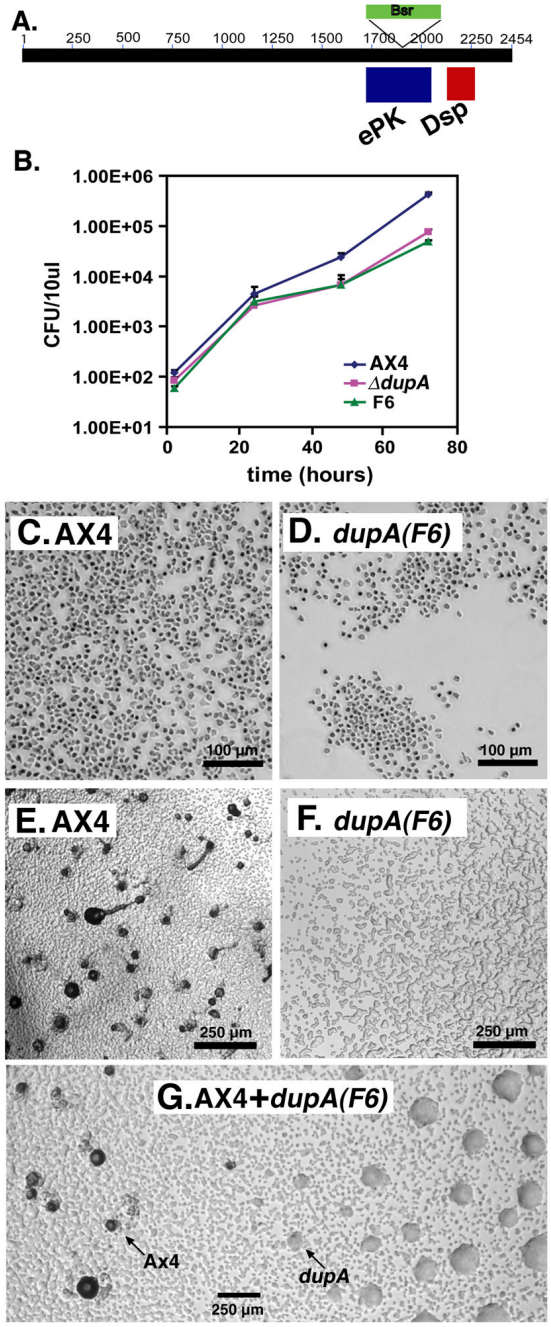

Figure 3. Reduced intracellular growth and developmental defects in a reconstructed *dupA* mutant

(A) DupA protein domains and the insertion site of Bsr^R. The protein contains a protein kinase (ePK) domain and a dual-specificity protein phosphatase (DSP) domain. **(B)** Deletion in *dupA* gene shows depressed *L. pneumophila* intracellular growth. The values are the mean of CFU from triplicate samples ± SD. **(C–G)** Developmental defect of RI6(*dupA(F6)*). **(C, D)** Micrographs of vegetatively growing AX4 and *dupA(F6)* cells. **(E, F)** Multicellular development of **(E)** AX4 and **(F)** the *dupA(F6)* mutant on nitrocellulose membranes. Images were grabbed from a dissecting microscope 30 h. after plating.

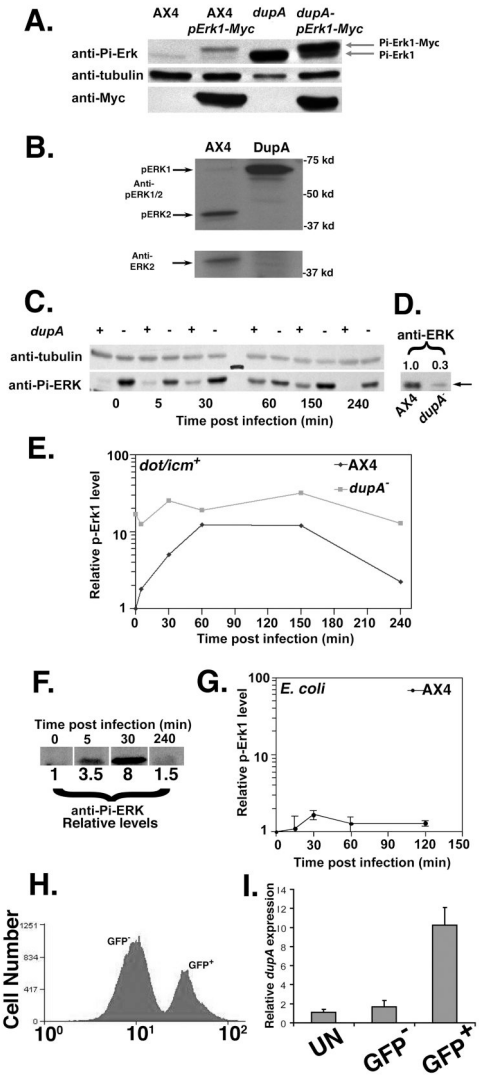

Figure 4. Control of ERK1 activation by DupA

(A) ERK1 is hyperphoshosphorylated in the *dupA*$^{-}$ mutant. Noted strains were transformed with plasmid expressing myc-tagged ERK1 (Experimental Procedures). **(B).** The absence of DupA results in ERK1 hyperphosphorylation and loss of ERK2. AX4(*dupA*$^{+}$) or the *dupA (F6)* were analyzed by Western blotting with either anti-phophoERK (top) or anti-ERK2 antibodies (bottom; Experimental Procedures) (Maeda et al., 2004). Bottom panel: blot in top panel was stripped and reprobed with anti ERK. **(C)** ERK1 is phosphorylated in response to *L. pneumophila* infection. *D. discoideum* were challenged with *L. pneumophila* for indicated times and 5×10^5 cells were analyzed by probing blots with anti-phospho-ERK (Experimental Procedures). **(D).** Reduced amount of ERK1 antigen in *dupA(F6)* mutant. Blot in panel C was stripped and reprobed with anti ERK (Experimental Procedures). Numbers above blot denote relative amount of antigen based on densitometry. **(E).** Disruption of *dupA* results in high level phosphorylation of ERK1. Bands were quantified by scanning densitometry of Western blots. Data are the mean of two samples. Experiment was performed 3 times. **(F)**. Increase in phospho-ERK1 in response to *L. pneumophila dotA3* strain. Relative phosphoERK1 levels determined by denstitometry. **(G).** Response of AX4 ERK1 phosphorylation to *E. coli* K12. Amoebae were challenged by *E. coli* at MOI = 1 and phosphorylation levels determined as in

panel E. Data are mean of three samples. **(H)** Isolation of AX4 population harboring *L. pneumophila* Lp01-GFP 8 h. post-infection. **(I)** Total RNA was isolated from each population and qPCR for *dupA* was performed. Relative *dupA* gene expression was normalized to uninfected cells (Experimental Procedures). N=3. Values are mean ± S.D.

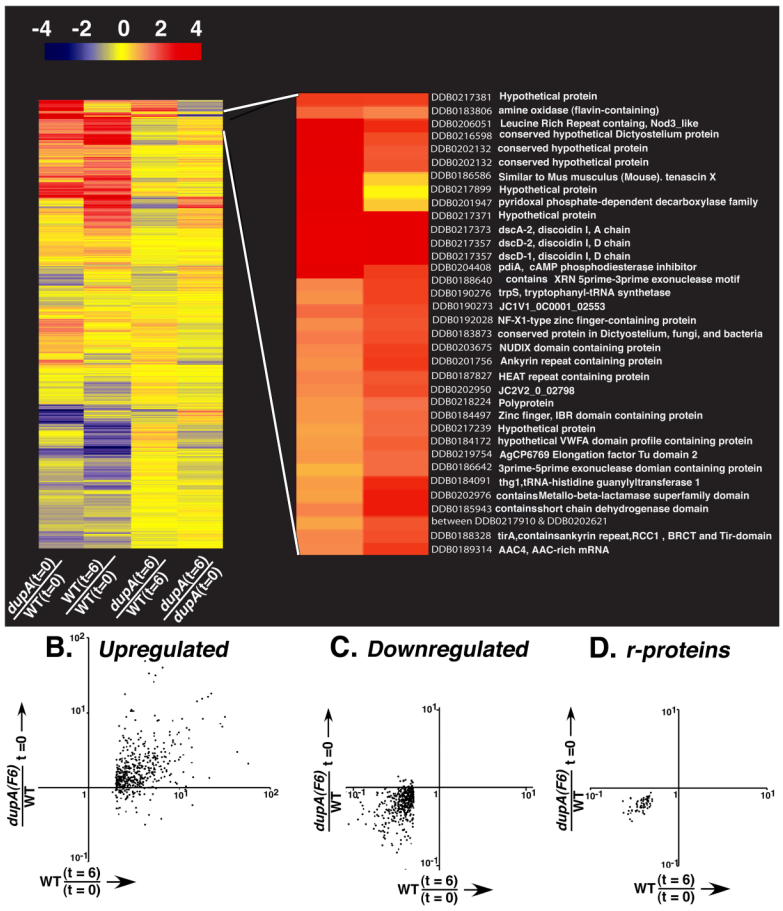

Figure 5. Microarray analysis of *dupA(F6)* mutant compared to *L. pneumophila challenged* AX4 strain

(A) Correlation cluster analysis of genes that had altered expression upon *L. pneumophila* infection or were altered in *dupA* in the absence of infection. Each condition is represented as the mean from microarrays from three independent infections. Enlarged is a small cluster of genes over-expressed in the *dupA*$^{-}$ mutant and induced in the infected AX4 cells. Comparison of AX4 to *dupA(F6)* mutant incubated in absence of bacteria: *dupA*(t=0)/WT(t=0). Comparison of AX4 incubated after 6 hrs infection compared to incubation in absence of bacteria: WT(t=6)/WT(t=0). Comparison of AX4 to *dupA(F6)* mutant incubated in presence of bacteria for 6 h.: *dupA*(t=6)/WT(t=6). *dupA(F6)* incubated after 6 hrs infection compared to incubation in absence of bacteria: *dupA*(t=6)/*dupA*(t=6). **(B)** A large fraction of the genes upregulated in AX4(WT) after *L. pneumophila* infection are overexpressed in the *dupA(F6)* mutant. **(C)** A large fraction of the genes downregulated in AX4(WT) in response to *L. pneumophila* are underexpressed in the *dupA(F6)* mutant. **(D)** Ribosomal protein genes are both downregulated in AX4(WT) in response to *L. pneumophila* and underexpressed in *dupA(F6).* See Supplemental Table 7 for individual data points.

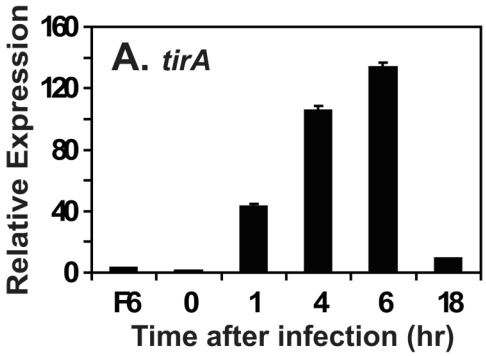

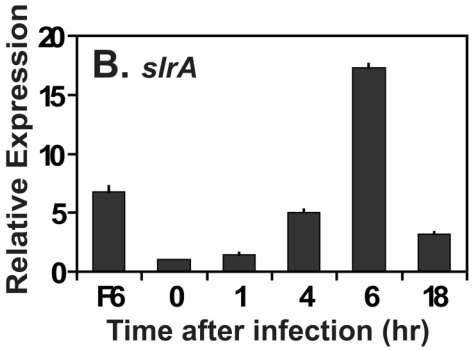

C.

DDB.ID	Annotation	WT (t=6)/(t=0) array	WT (t=6)/(t=0) qPCR	*dupA*(t=0)/WT (t=0) array	*dupA*(t=0)/WT (t=0) qPCR
DDB_G0275703	GefN	3.3	12	8.0	7.9
DDB_G0277863	PdiA	5.4	8.3	32	56
DDB_G0273919	Discoidin I	18	5.6	16	22
DDB_G0280575	Nod3	6.5	3.4	40	19

Figure 6. Upregulation of genes associated with an amoebal innate immune response after incubation with *L. pneumophila*

L. pneumophila LP01 was introduced onto monolayers of AX4(WT), and total RNA was prepared from the *D. discoideum* cells at time points noted. qPCR analysis of the either the *tirA* **(A)** or *slrA* genes **(B)** was determined from triplicate infections and expression level was plotted relative to uninfected WT. Data are mean ± S.E. Total RNA was also prepared from *dupA(F6)* in absence of infection and qPCR data are plotted relative to uninfected WT. **(C)** Verification of array data by qPCR (Experimental Procedures). Data are fold changes determined exactly as in panels 6A and 6B, performing qPCR at timepoints noted in each column. Both qPCR and array data are expressed as ratios at headers of each column.

Table 1

Disruption of *dupA* results in misregulation of genes that respond to *L. pneumophila* infection.

DDB.ID	Annotation (# of Genes)	*dupA* 0hours / WT 0hours	WT 6hours / WT 0hours	*dupA* 6hours / *dupA* 0hours
Protein Degradation				
Reduced Expression				
Various	**Papain proteinases (4 genes)**	0.19–0.30	0.17–0.32	0.67–1.17
DDB_G0290333	**Physarolisin**	0.49	0.39	0.65
Enhanced Expression				
DDB_G0278761	**La (Lon) serine protease**	4.43	2.93	0.75
Various	**IBR domain proteins (2 genes)**	2.6–4.3	3.6–8.4	1.20
DDB_G0267906	**OUT-like cysteine protease**	3.03	6.29	1.40
Various	**Proteosome subunits (2 genes)**	10.70	2.0–3.1	1.14
DDB_G0288093	**Ring finger proteins (3 genes)**	2.4–2.9	3.2–3.6	0.92–1.22
DDB_G0269462	**Ubiquitin family member**	2.46	3.06	1.17
DDB_G0288697	**Ubiquitin E2-4 enzyme**	2.01	5.50	1.82
Carbon metabolism				
Reduced Expression				
DDB_G0288289	**RliF; Beta-xylosidase**	0.49	0.18	0.26
DDB_G0278275	**Ribulose phosphate-3-epimerase**	0.36	0.26	0.62
DDB_G0272781	**Phosphomannomutase**	0.46	0.32	0.74
DDB_G0270018	**Dehydrogenase signature**	0.41	0.49	0.76
DDB_G0278341	**Citrate lyase b-subunit**	0.19	0.47	3.07
Enhanced Expression				
DDB_G0284277	**Dehydrogenase signature (2 genes)**	2.5–2.9	5.2–7.7	0.64–2.1
Nucleotide metabolism				
Reduced Expression				
DDB_G0281551	**GMP synthesis (2 genes)**	0.30–0.34	0.14-.30	0.23–0.45
DDB_G0280041	**Pyrimidine synthesis (2 genes)**	0.33–0.50	0.15–0.21	0.32–0.45
DDB_G0277725	**Methylenetetrahydrofolate dehydrogenase**	0.35	0.18	0.53
DDB_G0288333	**Purine synthesis (3 genes)**	0.27–0.43	0.21–0.40	0.55–0.81
DDB_G0280567	**CTP synthase**	0.45	0.19	0.55
Potential Immune response genes/antimicrobial proteins				
Enhanced Expression				
DDB_G0280575	**Nod3, Leucine-rich repeat signature**	40.31	6.49	0.42
DDB_G0289237	**TirA**	2.71	4.58	0.98
DDB_G0291083	**TirC**	2.30	3.99	1.18
DDB_G0290971	**TRAF-type zinc finger***	1.94	3.13	1.26
DDB_G0271590	**Antibiotic O-methyltransferase**	3.87	3.95	1.11
DDB_G0289149	**LPS induced TNF alpha Factor***	2.79	1.83	1.15
Protein Synthesis				
Reduced Expression				
DDB_G0281839	**WD domain, G-beta repeat**	0.43	0.20	0.77

DDB.ID	Annotation (# of Genes)	*dupA* 0hours / WT 0hours	WT 6hours / WT 0hours	*dupA* 6hours / *dupA* 0hours
DDB_G0279387	**Ribosomal proteins (8 genes)**	0.38–0.48	0.24–0.41	0.23–1.19
Enhanced Expression				
DDB_G0285725	**Deoxyhypusine synthase Probable**	3.65	3.54	1.06
DDB_G0283877	**Dihydrouridine synthase (Dus)**	4.03	6.72	1.65
DDB_G0280703	**EF-1 guanine nucleotide exchange**	8.31	17.91	1.61
DDB_G0292538	**Elongation factor Tu**	2.40	3.60	0.85
DDB_G0276493	**Eukaryotic translation initiation factor 6 (EIF-6)**	3.14	2.39	0.98
DDB_G0275625	**tRNAsynthetases (2 genes)**	2.5–3.9	5.0–10.3	1.3–1.7
Cell Adhesion/cytoskeleton				
Reduced Expression				
DDB_G0285793	**DdCAD-1 putative adhesion molecule**	0.39	0.49	0.43
Enhanced Expression				
DDB_G0285981	**von Willebrand factor domain (3 genes)**	2.5–2.6	5.5–7.05	1.1–1.2
Signal transduction				
Enhanced Expression				
DDB_G0284331	**3′,5′-cyclic-nucleotide phosphodiesterase regA**	11.07	2.96	0.74
DDB_G0269728	**CIA, Cytosolic Iron-sulfur protein Assembly**	5.18	9.39	0.97
DDB_G0273533	**Cyclic AMP receptor 1**	5.71	3.77	1.41
DDB_G0280339	**Cyclic nucleotide phosphodiesterase inhibitor related**	26.01	5.20	1.19
DDB_G0275703	**Ras guanine nucleotide exchange factor**	8.04	3.27	0.90
DDB_G0277863	**Cyclic nucleotide phosphodiesterase inhibitor PdiA**	31.65	5.41	1.20
DDB_G0287233	**Guanosine polyphosphate phosphohydrolase**	2.33	3.35	0.95
DDB_G0292160	**G-protein coupled-like receptor, possible**	2.56	3.24	0.95
Cell cycle				
Enhanced Expression				
DDB_G0292758	**Mob1/phocein family cell cycle protein**	2.82	3.67	0.99
DDB_G0278125	**Regulator of chromosome condensation.**	4.35	5.43	0.79
DDB_G0293756	**RCC1-containing domain**	2.95	3.00	0.83
Hydrolases/lipases				
Reduced Expression				
DDB_G0282371	**Hyaluronidase**	0.44	0.32	0.54
DDB_G0293460	**Calcineurin-like phosphoesterase (3 genes)**	0.29–0.45	0.35–0.40	0.74–1.3
DDB_G0274181	**Glycosyl hydrolases family 25**	0.27	0.41	0.91
DDB_G0268064	**Phospholipase/Carboxylesterase**	0.21	0.42	2.47
DDB_G0293566	**Lysozyme, putative**	0.23	0.45	1.13
Enhanced Expression				
DDB_G0290265	**DdFRP1alpha**	2.12	7.55	0.96
DDB_G0274291	**Similar to Bacteriophage T4 lysozyme**	2.38	2.03	0.85
DDB_G0290975	**Vegetative specific protein H5**	6.26	2.49	0.52
Nucleic Acid Interaction				

DDB.ID	Annotation (# of Genes)	*dupA* 0hours / WT 0hours	WT 6hours / WT 0hours	*dupA* 6hours / *dupA* 0hours
Reduced Expression				
DDB_G0281293	**Ribonuclease DdI, T2 family**	0.29	0.38	0.86
between_DDB_G0272334_and_DDB_G0272336	**Ribonuclease, putative**	0.49	0.45	0.81
Enhanced Expression				
DDB_G0275469	**Endonuclease V**	5.97	12.77	1.34
DDB_G0277705	**Ribonuclease HII**	2.89	5.03	1.16
DDB_G0269630	**IliI, IliK; TatD related Dnases**	3.5–6.3	12.0–13.7	1.25–1.96
DDB_G0289921	**XRN 5′-3′exonuclease N-terminus**	2.69	5.19	1.09
DDB_G0284255	**Zinc finger, C2H2 type, nucleic acid binding**	4.37	2.53	1.49
DDB_G0272048	**NUDIX hydrolase family signature**	2.64	5.31	1.34
DDB_G0269966	**DEAD box protein DDX1**	2.01	5.20	1.19
DDB_G0292618	**HhH-GPD superfamily base excision**	2.16	3.63	1.15
Transcriptional control				
Reduced Expression				
DDB_G0268920	**srfC; putative MADS-box transcription factor**	0.49	0.34	1.19
Enhanced Expression				
DDB_G0285057	**Sin3 associated polypeptide p18**	2.36	5.38	0.84
DDB_G0289319	**C-myb-like transcription factor**	2.35	2.33	1.21
DDB_G0293102	**Helix-turn-helix homeodomain**	2.07	5.07	1.89
DDB_G0286515	**Involucrin repeat, B-box zinc finger**	2.36	9.74	2.15
DDB_G0284103	**MybZ, homeodomain**	2.41	2.23	1.01
DDB_G0283917	**NAD-dependent deacetylase sirtuin 2**	2.04	3.16	1.51
DDB_G0293590	**NF-X1 type zinc finger**	2.65	4.34	1.24
DDB_G0293532	**STATc protein**	2.51	2.50	0.99
Membrane trafficking/lysosomal function				
Enhanced Expression				
DDB_G0274391	**Alpha-L-fucosidase precursor**	8.95	2.60	1.61
DDB_G0291998	**Alpha-N-acetylglucosaminidase**	3.00	4.57	2.27
DDB_G0288203	**HEAT repeat**	2.84	4.20	1.21
DDB_G0267440	**LimpC, CD36**	2.19	2.70	1.21
DDB_G0275413	**Vacuolar sorting protein 9 (VPS9)**	3.64	4.08	0.79
DDB_G0289485	**Vacuolin A1**	2.51	5.45	1.52
Lipid metabolism				
Reduced Expression				
DDB_G0275125	**B-like phospholipase (2 genes)**	0.16–0.19	0.34–0.36	1.12–1.52
DDB_G0286651	**Saposin-like type B**	0.35	0.24	0.55
Enhanced Expression				
DDB_G0273557	**DHHC zinc finger domain**	3.93	4.08	1.14
DDB_G0284353	**Oxysterol-binding protein**	5.65	7.81	2.62
DDB_G0272955	**Phytanoyl-CoA dioxygenase (PhyH)**	3.02	6.96	1.41
DDB_G0268890	**Saposin-like type B, region 2**	3.50	2.43	1.18

DDB.ID	Annotation (# of Genes)	*dupA* 0hours / WT 0hours	WT 6hours / WT 0hours	*dupA* 6hours / *dupA* 0hours
DDB_G0292668	**Terpenoid cylases/protein prenyltransferase**	4.97	2.38	1.01
Cell surface proteins of unknown function				
Reduced Expression				
DDB_G0289907	**EGF-like domain**	0.22	0.23	0.93
DDB_G0272434	**EGF domain,thrombomodulin signature**	0.35	0.49	0.76
DDB_G0286677	**Type III EGF-like signature (2 genes)**	0.26–0.33	0.22–0.25	0.98–1.43
Enhanced Expression				
DDB_G0273915	**IliE; Lectin/glucanase superfamily**	18.20	22.10	1.30
Transporters				
Reduced Expression				
DDB_G0267454	**ADP/ATP translocase, Mitochondrial**	0.43	0.18	0.27
DDB_G0287461	**ABC transporter AbcG3**	0.28	0.22	0.63
DDB_G0270720	**Major Facilitator Superfamily**	0.34	0.24	0.59
DDB_G0277515	**Permease family**	0.30	0.26	0.78
DDB_G0279301	**Sodium/calcium exchanger protein**	0.38	0.43	1.08
Enhanced Expression				
DDB_G0292986	**ABC transporters (3 genes)**	2.25–2.85	2.29–3.17	0.73–1.10
DDB_G0274661	**Phosphotransferase membrane protein**	2.21	2.73	1.39
DDB_G0292830	**sodium, hydrogen exchanger**	6.67	2.16	1.00
DDB_G0283345	**Sugar transporter ComD**	10.69	2.89	0.77
Development				
Reduced Expression				
DDB_G0281823	**V4-7,vegetative stage specific**	0.34	0.09	0.26
Enhanced Expression				
DDB_G0273919	**Discoidin I-like chains (2 genes)**	15.5–17.1	17.7–21.7	1.31–1.33
DDB_G0290925	**Similar to psiA, inducer of prespore cell division**	17.83	2.49	0.98
Detoxification				
Reduced Expression				
DDB_G0287229	**GMC oxidoreductase (choline dehydrogenase)**	0.24	0.40	1.38
Enhanced Expression				
DDB_G0273789	**Dyp-type peroxidase family**	2.65	6.81	1.53
DDB_G0291127		4.0–4.23	2.66	0.75–0.79

Either wild type *D. discoideum* AX4 or the *dupA(F6)* mutant were incubated in the presence (6 hours) or absence (0 hours) of *L. pnuemophila* in MB medium, RNA was extracted and microarrays were performed (Materials and Methods). Shown are array data from comparisons between: 1) infected AX4 and uninfected AX4 (WT 6 hours/WT 0 hours); 2) uninfected *dupA(F6)* mutant and infected AX4 (*dupA* 0 hours/WT 0 hours); 3) infected dupA (F6) and uninfected *dupA(F6) (dupA* 6 hours/*dupA 0* hours). The data are given as ratios of the expression levels of each gene between he two conditions, with the numerator and denominator as shown in the header for each column. Shown are fold ratios.